Measurements of Compact Intracloud Discharges with a Dense Array of Ground-Based Sensors

Sumedhe Karunarathe[1*], Thomas C. Marshall[1],Maribeth Stolzenburg[1], and Nadeeka Karunarathna[1]
[1]Dept. of Physics and Astronomy, University of Mississippi, University, Mississippi, U.S.A.

ABSTRACT: Compact intracloud discharges or narrow bipolar pulses (NBPs) are lightning discharges that occur during some thunderstorms and considered as singular, compact, high-energy, and high altitude events. During summer of 2011, we operated ten stations of wide band (band width 0.16 Hz – 2.5 MHz) electric field change meters covering an area of nearly 70×100 km^2 in and around Kennedy Space Center (KSC), Florida, USA. On 14 August 2011, we detected 244 positive polarity NBPs within 200 km of KSC. Analyzing E-change waveforms, we identified three main types of +NBPs, clean bipolar (5%), NBPs with secondary peaks (50%), and NBPs with faster risetime but longer duration (15%). Some NBPs (30%) were not classified using waveforms as they have extra wiggles in their waveforms. Locations of these NBPs were found with a Time of Arrival technique using the E-change waveforms detected at multiple sites. The altitudes of NBPs varied from 7 to 19 km with most of them occurring at about 13 km. The altitude distribution agrees well with findings from many prior studies. Temporal and spatial isolation of NBPs was found using their locations and occurrence times along with other location data such as LDAR2 and CGLSS. We found evidence of NBPs occurring just before, during, and just after lightning flashes and in isolation between flashes. In our data set, roughly 34.5% NBPs were isolated, 36.2% occurred just before flashes (within 660 ms) , 10.6% occurred just after flashes, and 18.7% occurred in the middle of lightning flashes. We obtained power spectral density curves for all NBPs and obtained the total RMS power radiated by NBPs in the frequency band of 1 kHz–2.5 MHz. The RMS power of NBPs had a wide range of 5.0×10^6–6.1×10^8 W with an average of 1.05×10^7 W.

INTRODUCTION

Narrow bipolar pulses (NBPs) or compact intracloud discharges (CIDs) were first reported by *Le Vine* [1980] as the most energetic lightning event in high and very high frequency bands. Some of the early analysis of NBPs using E-change and dE/dt recordings were done by *Willett et al.* [1989] and confirmed that NBPs are "relatively isolated and infrequent" as stated by *Le Vine* [1980]. The altitudes of NBPs are usually higher than most of the other lightning events [*Smith et al.*, 1999a, 2002, 2004]. A summary of altitudes and some other physical properties of NBPs observed at different parts of the world can be found in *Lü et al.* [2013]. Although the exact mechanism of NBPs is not clear, *Gurevich and Zybin* [2005] was the first to introduce a runaway electron avalanche process as a possible mechanism. Some modeling following this theory can be found in *Watson and Marshall* [2007] and *Cooray et al.* [2014]. Some of the NBPs have multiple secondary peaks [*Willett et al.*, 1989; *Hamlin et al.*, 2007]. *Nag and Rakov* [2010a,b] modeled those pulses and estimated electrical parameters using their "bouncing wave" model.

In this paper, we analyzed E-change data of 244 NBPs (or CIDs) recorded at multiple locations in and around Titusville, Florida and observed three main types of NBP waveforms according to their E-change waveforms. We discuss the physical properties of those NBPs and their types. We also do a power spectral density analysis of NBPs and discuss the RMS power radiated by NBPs in the frequency band of 1 kHz to 2.5 MHz.

---

*Corresponding author, email: skarunar@olemiss.edu, Postal address: 108 Lewis Hall, Dept. of Physics and Astronomy, University of Mississippi, University, MS 38655, U.S.A.

INSTRUMENTATIONS AND DATA

The data were collected in and around NASA/Kennedy Space Center (KSC), Florida in the summer of 2011. The primary data for this study came from E-change sensors placed at 10 different locations covering nearly 70 km $\times$ 100 km (Figure 1). Two types of E-change data are used here (1) ch3 data: decay time = 10 s, band width = 0.16 Hz – 2.6 MHz, Sampling frequency = 5 MHz, and vertical resolution = 12 bit. (2) ch1 data: decay time = 100 μs, band width = 1.6 kHz – 630 kHz, Sampling frequency = 1 MHz, vertical resolution = 12 bit. The detailed information about sensor placements and their operation can be found in *Karunarathne* [2013] and *Karunarathne et al.* [2013]. This array of E-change sensors have been used to determine the locations of initial breakdown pulses (IBPs) and return strokes [*Karunarathne et al.*, 2013; *Marshall et al.*, 2013, 2014] using time of arrival (TOA) technique called position by fast antenna (PBFA). Here we use PBFA to get the locations of NBPs.
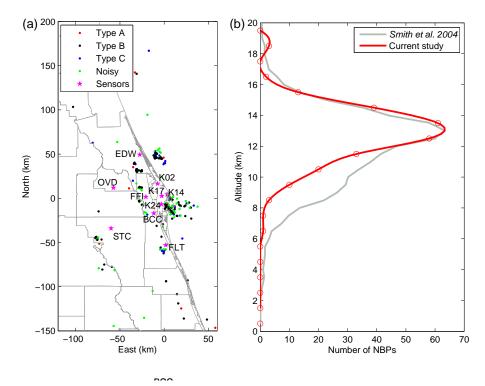

Figure 1: Locations of sensors and NBPs. (a) Sensor locations and their 3-character names are shown with pink asterisk. Horizontal locations of NBPs with color coded by their types are shown. (b) Altitude histogram on NBPs of current study (red curve) and that of *Smith et al.* [2004]. Note that horizontal data of *Smith et al.* [2004] curve was scaled by 0.0387 to match the peak of the current study.

We use data from LDAR2 (Lightning Detection And Ranging II, also called 4DLSS) which is described by *Thomas et al.* [2004] as a commercial version of the more well-known Lightning Mapping Array, or LMA [*Rison et al.*, 1999]. LDAR2 provides the locations of some fast lightning events. We also use data from CGLSS (Cloud-to-Ground Lightning Surveillance System) [*Wilson et al.*, 2009, e.g.,] which provides the locations of return strokes.

Throughout this paper, we use the Physics sign convention, where an upward positive electric field exerts an upward force on a positive charge. We use a Cartesian coordinate system with the origin coincident with LDAR2 origin where latitude and longitude were 28 32 18.55N and 80 38 33.48W respectively. In this

study we are focusing on 244 NBPs that were chosen from the data collected on Aug. 14th, 2011. All of these pulses are positive narrow bipolar pulses, meaning the initial half cycle of the bipolar pulse is positive.

OBSERVATIONS

Waveshapes

The E-change waveforms of NBPs were analyzed at multiple locations, and we have identified 3 main types of E-change waveforms associated with CIDs. Examples for each category are shown in Figure 2. Type A: In this group of pulses, we observe relatively clean bipolar pulses in every sensor. Examples for such pulses can be also found in *Eack* [2004]; 5% of our CID waveforms belong to this category. Type B: These pulses have one or more secondary positive peaks other than the main positive peak. Most (50%) of the NBP waveforms we analyzed belong to this category; examples of these types of waveforms can be found in *Willett et al.* [1989]; *Hamlin et al.* [2007]; *Nag and Rakov* [2009]. Type C: These pulses have relatively sharp rise and have a noisy tail that looks somewhat similar to return stroke (but the total duration is much shorter than a return stroke). Examples for such a pulse can be found in *Cooray and Lundquist* [1985]; *Willett et al.* [1989]; 15% of our data contains these kinds of pulses. The rest of the pulses were noisier and therefore it could not be determined whether they were related to above groups or to new groups using waveforms alone. However, using power spectrum density curves, we could include remaining noisier pulses into the above 3 groups as explained later.
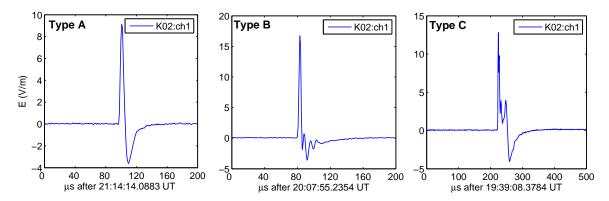

Figure 2: Types of NBP E-change waveshapes.

Locations

Locations of NBPs were obtained using a time of arrival technique known as position by fast antenna (PBFA) [*Karunarathne et al.*, 2013]. The horizontal locations of NBPs (relative to the LDAR2 origin) were from 10 km to 170 km with an average of 45 km. Altitudes of NBPs ranged from roughly 6-20 km (relative to mean sea level) and are in good agreement with the altitude histogram presented by *Smith et al.* [2004]. Horizontal locations of all NBPs and altitude histogram are shown in Figure 1.

Peak currents

We calibrated our E-change meters with the CGLSS system to obtain the estimations of peak currents [*Karunarathne*, 2013]. Assuming the NPBs had vertically oriented currents, the peak currents were estimated to range from 2 kA to 126 kA with an average of (30±20) kA with most of the values falling within 10–40 kA (Figure 3). These values are in agreement with *Eack* [2004] estimation of 24 kA. *Smith et al.* [1999a] estimated that the peak currents of their NBPs should be in the order of 280 kA but stated that this

value could be "physically unrealistic". Most of the values we estimated are an order of magnitude smaller than those in *Smith et al.* [1999a]. *Watson and Marshall* [2007] estimated peak currents >420 kA and *Nag and Rakov* [2010b] obtained arithmetic mean of 143 kA via modeling.
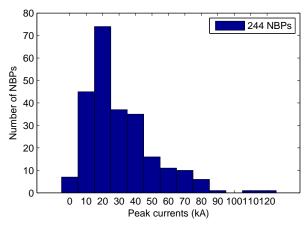

Figure 3: Distribution of peak currents.

Isolation

Locations of NBPs along with the locations of other lightning events (using PBFA, LDAR, and CGLSS) were used to find how isolated they are in space and time. Considering all the lightning events occurred within 10 km radius of a NBP, the temporally closest lightning events occurred before and after the NBP were defined as 'pre pulse' and 'post pulse' times (e.g., Figure 4). Histograms of pre and post pulse times are shown in Figure 5a and 5c. Since most of our lightning event occurred before, during, or after IC events rather than CG events, we use the mean flash duration of Florida IC flashes, 660 ms [*Bils et al.*, 1988], as a threshold to determine if a NBP is a part of a IC flash. With this threshold, if a lightning pulse occurred within 660 ms of NBP, we consider that NBP is related to that flash.

As shown in Figure 5b, roughly 34.5% of NBPs were truly isolated, meaning that there was no evidence of other lightning events occurring within a 10 km radius and a ±660 ms time interval from the NBP event (dark green region). 18.7% of NBPs has flashes both before and after within the threshold time as shown in white area. On the other hand, only 10.6% of NBPs occurred at the end of the lightning events (light green area) meaning that there are lightning events happening before the NBP (within the threshold) but no lightning events happening after the NBP event. However the biggest percentage, 36.2%, of NBPs had lightning happening within 660 ms after the NBP (purple region) meaning that there were no lightning events within 660 ms before the NBP event but there were some lightning events happening after the NBP event. We further found that about 29% of CIDs occurred before and within 50 ms of the initial stage of an IC flash, while less than 8% occurred after and within 100 ms of the end of an IC flash.

Altogether, since only 34.5% of NBPs were isolated, the rest 65.5% of the NBPs would be close to other lightning events within 660 ms temporally and 10 km spatially.

Power densities

Power spectral density (PSD) curves were obtained for all the NBPs at different sensors. Two preprocessing steps were used for E-change data before obtaining PSD curves. (1) A 1000 Hz digital high-pass filter was applied to filter out low frequency drifting and (2) data were normalized to 100 km using $1/R$ relation because NBP waveforms are dominated by radiation field [*Willett et al.*, 1989] for most of our cases.
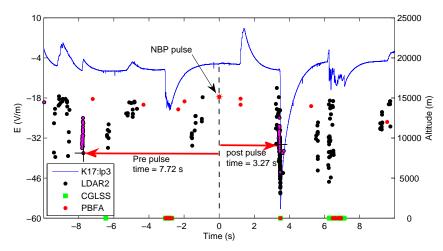
4

Figure 4: An illustration of 'pre pulse' and 'post pulse' times. The figure shows ±10 s data around a NBP detected at 70882.857949 UT shown with a red asterisk. Left vertical axis shows the 10 kHz continuous E-change recording of K17 sensor (blue line) while right hand axis shows the altitudes of the locations shown in colored dots. Purple dots are the lightning events occurred within 10 km radius of the NBP pulse. Note that during pre pulse time there are many other events occurring (black and red dots) but they were considered as not related to the NBP event because they are more than 10 km away from it.
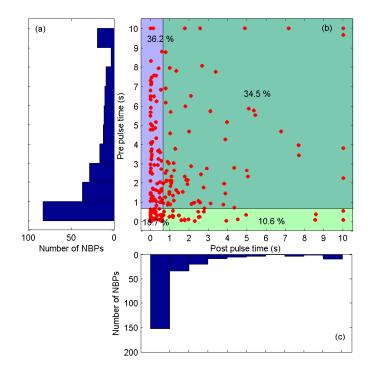

Figure 5: Distribution of pre pulse times and post pulse times. (a) Histogram of pre pulse times (b) cross figure of pre and post pulse times. Colored regions are defined considering 660 ms threshold explained in the text. (c) Histogram of post pulse times.

Usually, sensors within 30 km of NBPs were not used to make sure we are using only radiation field. Simi-

larly, sensors beyond 100 km were not used because of their signal to noise ratio is lower. Remaining PSD curves were averaged to obtain the final PSD curve for a given NBP.
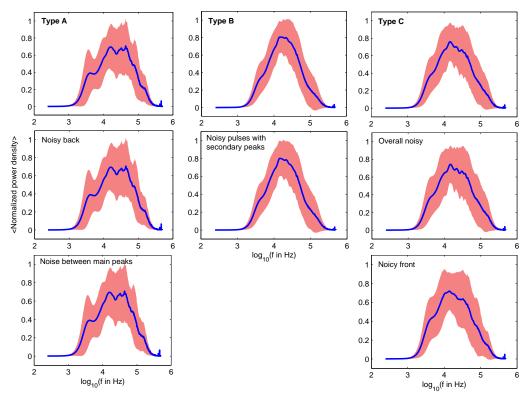

Figure 6: Normalized mean PSD curves (blue) of different types of NBPs. The standard deviation of each curve is shown with red shaded area. Top row shows the mean PSD curves for the main 3 types of NBPs found with waveform analysis. Remaining PSD curves are for the noisy NBPs that could not categorized earlier from waveform analysis.

Individual PSD curves were normalized to 1 and then averaged to obtain mean PSD distribution of different NBP types explained previously. Mean PSD curves and their standard deviations are shown in Figure 6. According to the wave shape analysis explained previously, we found 3 main types of NBPs. However 30% of NBPs could not be categorized as they were noisier, meaning they had extra wiggles somewhere in the pulse. However, we categorized them according to where the extra wiggles appeared and came up with 5 sub categories which are noisy front, noisy back, noise in between main peaks, overall noisy, and noisy pulses with secondary peaks. It is interesting to notice that the PSD curves of these sub categories are very similar PSD curves of one of the main categories. As shown in Figure 6, NBPs with noisy back and noise between main peaks had similar PSD curves as Type A, relatively clean, NBPs. It may be not surprising that noisy pulses with secondary peaks had a similar PSD curve as Type B, pulses with secondary peaks. Pulses with noisy front and noisy overall had similar PSD curves as Type C.

To obtained the total RMS power output of a NBP in our data recording band from 1 kHz (set by the digital high-pass filter) to 2.5 MHz (the Nyquist frequency), the integral of the PSD over the all frequencies was computed. Figure 7 shows the power distribution of all NBPs. RMS power values ranged from 5.0×10^6 W to 6.1×10^8 W. According to the Gaussian best fit for histogram, the average RMS power of NBPs was $10^{(7.02\pm0.56)}$ W. These values are smaller than the average peak current values reported by *Krider and Guo* [1983] for first and subsequent RSs given as $(2 \pm 2)\times 10^{10}$ W and $(3 \pm 4) \times 10^9$ W respectively.
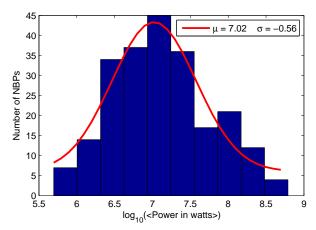
Figure 7: RMS power histogram of NBPs over the frequency range of 1 kHz-2.5 MHz. Gaussian best fit curve for the power histogram is shown in red. According to the best fit curve, the average RMS power of NBPs was $10^{(7.02\pm0.56)}$ W.

SUMMARY

We analyzed 244 +NBP E-change waveforms obtained at 10 different locations in and around Kennedy Space Center in Florida on Aug. 14, 2011. Based on the E-change waveforms we identified 3 main types of NBPs (and percent of the total), Type A: smooth NBPs (5%), Type B: NBPs with secondary peaks (50%), and Type C: NBPs with faster rise time but longer total duration (15%). The rest (30%) of the pulses had extra noise which prevented us from categorizing them in any of the above groups. However, after doing PSD curve analysis, we found that these remaining pulses also seem to belong to one of the three types described.

We obtained the locations of these +NBPs using fairly dense set (covering nearly 70×100 km^2 area) of 10 E-change meters and the TOA method described in *Karunarathne et al.* [2013]. The xy locations of NBPs near KSC (within 30 km horizontally from the origin) were usually accurate within 100 m while altitude error was usually < 500 m. Our altitude distribution of NBPs are in agreement of previous studies [*Smith et al.*, 1999a, 2002, 2004; *Wang et al.*, 2012; *Lü et al.*, 2013] and the upper part of the altitude histogram (Figure 1b) closely follow *Smith et al.* [2004] findings including the altitude of the majority of NBPs found at roughly 13 km.

We calibrated our system with CGLSS to obtain the peak currents of return strokes and the method was extended to obtain peak currents of cloud events [*Karunarathne*, 2013]. The peak current values ranged 2–126 kA with an average of 30 kA. The average value is in agreement with *Eack* [2004] findings but lower than most of the other studies [*Smith et al.*, 1999a; *Watson and Marshall*, 2007; *Nag and Rakov*, 2010b]. One of the reasons for under estimated peak currents could be the way we perform the calibration which was really intended for finding the peak currents of return strokes.

Narrow bipolar pulses are considered as isolated events *Le Vine* [1980]; *Willett et al.* [1989]. However, our current data set shows only 34.5% of NBPs are really isolated meaning that there were no other lightning events occurring within 10 km of NBPs and within ±660 ms, the mean duration of Florida lightning [*Bils et al.*, 1988]. Other 65.5% NBPs are closer to other lightning flashes specially within 10 km and temporally within 660 ms. *Wang et al.* [2012] also reported low percentage of (13.6%) NBPs were really isolated while others (86.4%) associated with either IC or CG lightning discharges.

Power spectral density and RMS power values of NBPs were obtained in the frequency band of 1 kHz–2.5 MHz. The three different types of the NBPs each had a characteristic PSD curve (Figure 6),

and we used PSD curves of NBPs that we could not categorize (due to appearance of extra peaks in E-change waveforms) to categorize them into the three main groups. RMS power values had a wide range of 5.0×10^6–6.1×10^8 W with an average of 1.05×10^7 W.

References

Bils, J. R., E. M. Thomson, M. A. Uman, and D. Mackerras (1988), Electric field pulses in close lightning cloud flashes, *Journal of Geophysical Research: Atmospheres (1984–2012)*, *93*(D12), 15,933–15,940.

Cooray, V., and S. Lundquist (1985), Characteristics of the radiation fields from lightning in sri lanka in the tropics, *Journal of Geophysical Research: Atmospheres*, *90*(D4), 6099–6109, doi:10.1029/JD090iD04p06099.

Cooray, V., G. Cooray, T. Marshall, S. Arabshahi, J. Dwyer, and H. Rassoul (2014), Electromagnetic fields of a relativistic electron avalanche with special attention to the origin of lightning signatures known as narrow bipolar pulses, *Atmospheric Research*.

Eack, K. B. (2004), Electrical characteristics of narrow bipolar events, *Geophys. Res. Lett.*, *31*, L20102, doi:10.1029/2004GL021117.

Gurevich, A. V., and K. P. Zybin (2005), Runaway breakdown and the mysteries of lightning, *Phys. Today*, *58*, 37–43.

Hamlin, T., T. E. Light, X. M. Shao, K. B. Eack, and J. D. Harlin (2007), Estimating lightning channel characteristics of positive narrow bipolar events using intrachannel current reflection signatures, *Journal of Geophysical Research: Atmospheres*, *112*(D14), n/a–n/a, doi:10.1029/2007JD008471.

Karunarathne, S. (2013), Numerical modeling of lightning initiation and stepped leader propagation, Ph.D. dissertation, The University of Mississippi, Oxford, MS, United States.

Karunarathne, S., T. C. Marshall, M. Stolzenburg, N. Karunarathna, L. E. Vickers, T. A. Warner, and R. E. Orville (2013), Locating initial breakdown pulses using electric field change network, *Journal of Geophysical Research: Atmospheres*, pp. 1–13, doi:10.1002/jgrd.50441.

Krider, E. P., and C. Guo (1983), The peak electromagnetic power radiated by lightning return strokes, *Journal of Geophysical Research: Oceans*, *88*(C13), 8471–8474, doi:10.1029/JC088iC13p08471.

Le Vine, D. M. (1980), Sources of the strongest rf radiation from lightning, *Journal of Geophysical Research: Oceans (1978–2012)*, *85*(C7), 4091–4095.

Lü, F., B. Zhu, H. Zhou, V. A. Rakov, W. Xu, and Z. Qin (2013), Observations of compact intracloud lightning discharges in the northernmost region (51 n) of china, *Journal of Geophysical Research: Atmospheres*, *118*(10), 4458–4465.

Marshall, T., M. Stolzenburg, S. Karunarathne, S. Cummer, G. Lu, H.-D. Betz, M. Briggs, V. Connaughton, and S. Xiong (2013), Initial breakdown pulses in intracloud lightning flashes and their relation to terrestrial gamma ray flashes, *Journal of Geophysical Research: Atmospheres*, *118*(19), 10,907–10,925, doi:10.1002/jgrd.50866.

Marshall, T., W. Schulz, N. Karunarathna, S. Karunarathne, M. Stolzenburg, C. Vergeiner, and T. Warner (2014), On the percentage of lightning flashes that begin with initial breakdown pulses, *Journal of Geophysical Research: Atmospheres*, *119*(2), 445–460, doi:10.1002/2013JD020854.

Nag, A., and V. A. Rakov (2009), Electromagnetic pulses produced by bouncing-wave-type lightning discharges, *IEEE Transactions on Electromagnetic Compatibility*, *50*(03), 466–470.

Nag, A., and V. A. Rakov (2010a), Compact intracloud lightning discharges: 1.mechanism of electromagnetic radiation and modeling, *J. Geophys. Res.*, *115*, D20102, doi:10.1029/2010JD014235.

Nag, A., and V. A. Rakov (2010b), Compact intracloud lightning discharges: 2.estimation of electrical parameters, *J. Geophys. Res.*, *115*, D20103, doi:10.1029/2010JD014237.

Rison, W., R. J. Thomas, P. R. Krehbiel, T. Hamlin, and J. Harlin (1999), A gpsbased threedimensional lightning mapping system: Initial observations in central new mexico, *Geophys. Res. Lett.*, *26(23)*, doi:10.1029/1999GL010856.

Smith, D., K. Eack, J. Harlin, M. Heavner, A. Jacobson, R. Massey, X. Shao, and K. Wiens (2002), The los alamos sferic array: A research tool for lightning investigations, *Journal of Geophysical Research: Atmospheres (1984–2012)*, *107*(D13), ACL–5.

Smith, D. A., X. M. Shao, D. N. Holden, C. T. Rhodes, M. Brook, P. R. Krehbiel, M. Stanley, W. Rison, and R. J. Thomas (1999a), A distinct class of isolated intracloud lightning discharges and their associated radio emissions, *Journal of Geophysical Research: Atmospheres*, *104*(D4), 4189–4212, doi:10.1029/1998JD200045.

Smith, D. A., M. J. Heavner, A. R. Jacobson, X. M. Shao, R. S. Massey, R. J. Sheldon, and K. C. Wiens (2004), A method for determining intracloud lightning and ionospheric heights from vlf/lf electric field records, *Radio Science*, *39*(1), n/a–n/a, doi:10.1029/2002RS002790.

Thomas, R. J., P. R. Krehbiel, W. Rison, S. J. Hunyady, W. P. Winn, T. Hamlin, and J. Harlin (2004), Accuracy of the Lightning Mapping Array, *J. Geophys. Res.*, *109*, D14207, doi:10.1029/2004JD004549.

Wang, Y., G. Zhang, X. Qie, D. Wang, T. Zhang, Y. Zhao, Y. Li, and T. Zhang (2012), Characteristics of compact intracloud discharges observed in a severe thunderstorm in northern part of china, *Journal of Atmospheric and Solar-Terrestrial Physics*, *84*, 7–14.

Watson, S. S., and T. C. Marshall (2007), Current propagation model for a narrow bipolar pulse, *Geophysical Research Letters*, *34*, L04816, doi:10.1029/2006GL027426.

Willett, J. C., J. C. Bailey, V. P. Idone, A. Eybert-Berard, and L. Barret (1989), Submicrosecond intercomparison of radiation fields and currents in triggered lightning return strokes based on the transmission-line model, *J. Geophys. Res.*, *94*, D11, doi:10.1029/JD094iD11p13275.

Wilson, J. G., K. L. Cummins, and E. P. Krider (2009), Small negative cloud-to-ground lightning reports at the nasa kennedy space center and air force eastern range, *J. Geophys. Res.*, *114*, D24103, doi:doi:10.1029/2009JD012429.